UNVEILING OLIVINE ON VESTA USING VIR DATA AND USGS CARTOGRAPHIC SOFTWARE.

J. R. Heup[1] and T. Titus[2], [1]University of Wisconsin-Madison (heup@wisc.edu), [2]USGS Astrogeology Science Center, 2255 North Gemini Dr., Flagstaff, AZ 86001 (ttitus@usgs.gov).

Introduction: The Dawn spacecraft orbited the asteroid 4 Vesta (hereafter referred to as Vesta) from July 16, 2011 until September 5, 2012 [1]. During that time, it acquired data with three instruments: The Framing Camera (FC) [2], the Visual and InfraRed spectrometer (VIR) [3], and the Gamma Ray and Neutron Detector (GRaND) [4]. Our goal was to use USGS cartographic software, the Integrated System for Imagers and Spectrometers (ISIS), to process and analyze the Dawn VIR data in order to determine whether we could detect olivine on Vesta's surface.

Data: We selected two craters on Vesta's northern hemisphere, Arruntia and Bellicia, for analysis. These craters were selected because they are relatively large (approximately 10 km and 42 km in diameter, respectively), they are close together, and they have already been identified as likely containing olivine [5]. Four image cubes of Arruntia and six of Bellicia were acquired from the Planetary Data System (PDS). To analyze mineralogy, we used 44 spectra of different mixtures of olivine (OL), low- and high-calcium pyroxene (LCP, HCP, respectively), and plagioclase (PLG), acquired from RELAB [http://www.planetary.brown.edu/relabdata/].

Methods: Within ISIS we created two sets of uncontrolled mosaics. The first was a hyperspectral mosaic of the entire VIR spectra.

Fig. 1 Hyperspectral mosaics of Arruntia (left) and Bellicia (right). The channels red, green, and blue are 1.957 µm, 9.0 µm, and 0.687 µm, respectively.

The second was a band index mosaic, which isolated the normalized band depth of the 0.9 µm and 1.9 µm absorption bands (BI and BII, respectively). We then identified five endmembers based on the colors in the band index mosaics (Fig. 2): "green", "blue", "yellow", "light gray", and "dark gray". The "green" region was of particular interest because it indicates a large difference between the BI and BII depths, and because it appears to correspond to areas where olivine has been previously identified [1].

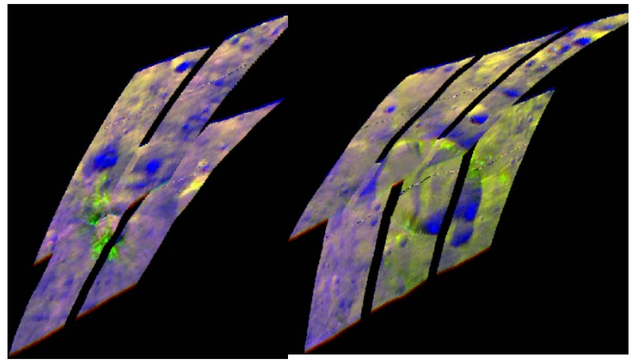

Fig. 2 Band index mosaics of Arruntia (left) and Bellicia (right). The channels red, green, and blue are BII, BI/BII, and BI, respectively.

Results: Two methods were used to analyze the mineralogy of these craters: (1) comparing the ratios of the BI and BII depths and (2) doing a best fit analysis of the spectra in IDL (Fig. 3).

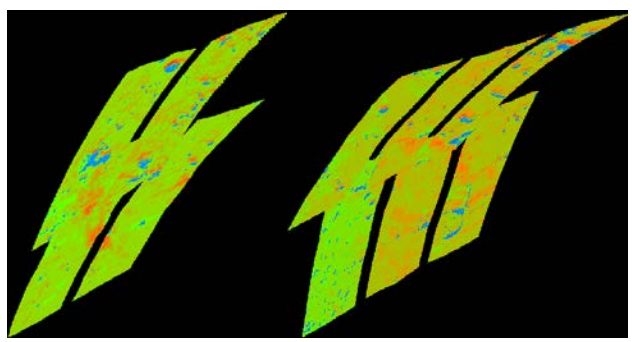

Fig. 3 Mineral maps of Arruntia (left) and Bellicia (right). The channels red, green and blue are olivine, high- and low-calcium pyroxene, and plagioclase, respectively.

Band Depth Ratios: The band depth ratio analysis found different mixtures with varying levels of olivine for each endmember, but there were discrepancies between Arruntia and Bellicia's results. Arruntia's "green" and "dark gray" regions were found to be high in olivine, while the "light gray" and "blue" regions were less so, and the "yellow" region contained no olivine. For Bellicia, it was the "dark gray" region that was high in olivine, while the “light gray” and “blue” contained lesser amounts and both the green and yellow regions showed no olivine. These discrepancies are most likely due to a mixture of mineral types at the pixel scale combined with a limited spectral library of only 44 samples.

Spectral Best-fit Method: The best fit analysis, which tried to fit much of the spectra shortward of 2.4 μm, showed that the “green” regions of both craters are consistent with the presence of olivine. The “yellow”, “light gray”, and “dark gray” areas are a mixture of LCP and HCP, while the “blue” areas may contain PLG. Fig. 4 shows a comparison of a spectrum from the “green” region to RELAB spectra of olivine, and high- and low-calcium pyroxene. BII normalized band ratio is extremely shallow compared to BI normalized band ratio (consistent with olivine) but the BI band center is more consistent with low-calcium pyroxene than with olivine. This inconsistency suggests either a mixture of olivine and pyroxene or different type of olivine (Fe-Mg content) on the surface than was used in the RELAB spectral library.

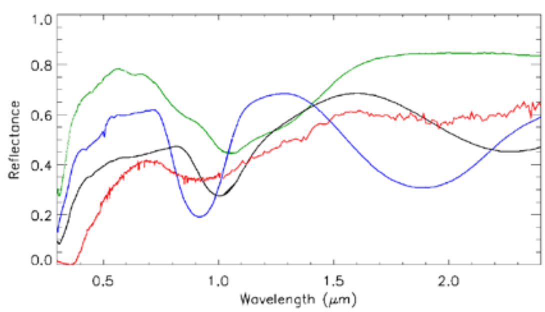

Fig. 4 Spectrum from the “green” region of Arruntia (red) compared to RELAB spectra of olivine (green), low-calcium pyroxene (blue) and high-calcium pyroxene (black).

Conclusions: The band index mosaics allowed us to identify a “green” endmember which we suspected contained olivine. Although an analysis of band depth ratios proved inconclusive, a best fit analysis suggests that the “green” endmember does contain olivine. Furthermore, the locations of the green endmember corresponds well to the locations where olivine has been identified in the two craters [1]. ISIS has proven to be a useful tool for analyzing Dawn VIR data.

Future Work: While the USGS ISIS software package has the capability to produce hyperspectral and band-index mosaics from the Dawn VIR data, the ability to control those mosaics is not currently available. This limitation had minimal impact for this study, but will prevent the creation of usable global hyperspectral mosaics of Vesta in the near future.

The addition of the Modified Gaussian Method [6] to the suite of ISIS applications would also greatly increase the spectral analysis capabilities.

The pilot study used a small spectral library with only one type of olivine. The size of the library needs to be expanded – adding several additional types of olivine. Additional minerals, such as glass, may also need to be added.

Acknowledgments: We would like to thank the Northern Arizona University Research Experience for Undergraduates supporting this research. We would also like to recognize Tammy Becker, whose knowledge and expertise with ISIS proved to be a valuable resource that greatly contributed to the success of this project. This abstract contributed greatly from insightful comments from Laszlo Kestay.

References:

[1] Russell, C. T. et al. (2013) *Meteoritics & Planetary Science*, **48**(11), 2076-2089. [2] Sierks et al. (2011) *Space Sci. Rev.*, **163**, 263 [3] De Sanctis M. C. (2011) *Space Sci. Rev.*, 163:329–369. [4] Prettyman T. H. et al. (2012) Sci., 338, 242-246. [5] Thangjam, G. et al. (2014) *Meteoritics & Planetary Science*, *49*(10; 10), 1831-1850. [6] Sunshine, J. and Pieters, C. M. (1993) *JGR*, **98**, 9075-9087.